

Synthesis of polysulfone beads impregnated with Ca-sepiolite for phosphate removal

Seung-Hee Hong^{1a}, Chang-Gu Lee^{2b}, Sanghyun Jeong^{3c} and Seong-Jik Park^{*4}

¹Department of Integrated System Engineering, Hankyong National University, Anseong, 17579, Republic of Korea

²Department of Environmental and Safety Engineering, Ajou University, Suwon 16499, Republic of Korea

³Department of Environmental Engineering, Pusan National University, Busan, 46241, Republic of Korea

⁴Department of Bioresources and Rural System Engineering, Hankyong National University, Anseong, 17579, Republic of Korea

(Received October 29, 2019, Revised December 3, 2019, Accepted December 4, 2019)

Abstract. Former studies revealed that sepiolite thermally treated at high temperature have high adsorption capacity for phosphate. However, its micron size (75 μm) limits its application to water treatment. In this study, we synthesized sepiolite impregnated polysulfone (PSf) beads to separate it easily from an aqueous solution. PSf beads with different sepiolite ratios were synthesized and their efficiencies were compared. The PSf beads with 30% impregnated sepiolite (30SPL-PSf bead) possessed the optimum sepiolite ratio for phosphate removal. Kinetic, equilibrium, and thermodynamic adsorption experiments were performed using the 30SPL-PSf bead. Equilibrium adsorption was achieved in 24 h, and the pseudo-first-order model was suitable for describing the phosphate adsorption at different reaction times. The Langmuir model was appropriate for describing the phosphate adsorption onto the 30SPL-PSf bead, and the maximum adsorption capacity of the 30SPL-PSf bead obtained from the model was 24.48 mg-PO₄/g. Enthalpy and entropy increased during the phosphate adsorption onto the 30SPL-PSf bead, and Gibb's free energy at 35 °C was negative. An increase in the solution pH from 3 to 11 induced a decrease in the phosphate adsorption amount from 27.30 mg-PO₄/g to 21.54 mg-PO₄/g. The competitive anion influenced the phosphate adsorption onto the 30SPL-PSf bead was in the order of NO₃⁻ > SO₄²⁻ > HCO₃⁻. The phosphate breakthrough from the column packed with the 30SPL-PSf bead began after ~2000 min, reaching the influent concentration after ~8000 min. The adsorption amounts per unit mass of 30SPL-PSf and removal efficiency were 0.775 mg-PO₄/g and 61.6%, respectively. This study demonstrates the adequate performance of 30SPL-PSf beads as a filter for phosphate removal from aqueous solutions.

Keywords: sepiolite; polysulfone; beads; phosphate; adsorption

1. Introduction

Phosphorus is an essential nutrient for all living organisms. It is used for synthesizing genetic materials (deoxyribonucleic acid and ribonucleic acid), the structure of cells (phospholipids) and bones (hydroxyapatite), and energy transfer (adenosine triphosphate) (Ruttenberg 2003). Furthermore, phosphorus is a key component of fertilizers for agricultural cultivation. However, high concentrations of phosphorus in rivers result in eutrophication, which stimulates algal blooms and promotes hypoxic or anoxic conditions (Mallin *et al.* 2006, Gao *et al.* 2013, Petkuvienė *et al.* 2016). To prevent excess phosphorus in water bodies, the Korean government enforced the standards for the total phosphorus (TP) in effluents discharged directly from wastewater treatment plants in 2012, and the TP concentrations were set at 0.2, 0.3, and 0.5 mg/L for districts I, II, and III, respectively (Kang *et al.* 2017).

Various technologies have been applied for the removal of phosphate from wastewater, including chemical precipitation, constructed wetlands, electrodialysis, reverse osmosis, membrane filtration, biological methods, ion exchange, and adsorption (Loganathan *et al.* 2014). Although the biological wastewater treatment method is the most widely used in wastewater treatment plants globally, the lowest level of phosphorus concentration after biological treatment has been reported to be 1 mg/L (Clark *et al.* 2005). The amount of phosphorus removed by biological treatment also depends on temperature; it increases and decreases with the temperature (Ramasahayam *et al.* 2014). The biological treatment requires a post-process to meet the newly enforced discharge standards. Adsorptive filtration is a widely used method for water treatment due to its low cost, low energy consumption, and ease of operation (Park *et al.* 2015).

The cost and efficiency of adsorptive filtration depend heavily on the adsorbents, and low-cost adsorbents with high removal capacity for target contaminants have been investigated by many researchers. Metals (Fe, Al, and Zr) (hydro)oxide, calcium and magnesium carbonates, clay minerals (vesuvianite, montmorillonite, bentonite, and layered double hydroxides), activated carbon, anion exchange resins, and industrial byproducts (red mud, fly ash, slags, and biological wastes) have been used as adsorbents

*Corresponding author, Associate Professor

E-mail: parkseongjik@hknu.ac.kr

^a Ph.D. Candidate

^b Assistant Professor

^c Assistant Professor

for the removal of phosphate from water and wastewater (Loganathan *et al.* 2014, Ramasahayam *et al.* 2014, Kim *et al.* 2019). Although most clay minerals do not have high efficiency for the removal of anions including phosphate owing to their negative charges (Loganathan *et al.* 2014), sepiolite has been reported to have a high adsorption capacity for phosphorus in other literature (Yin *et al.* 2011). Moreover, sepiolite is an inexpensive (0.4–0.6 \$/kg) and abundant natural clay mineral (Yin *et al.* 2013, Liu *et al.* 2018); thus, it is considered as a promising adsorbent for phosphate removal from wastewater. However, its micro size limits its application under continuous flow conditions.

In this study, we suggest the use of sepiolite by impregnating it with polysulfone (PSf) beads to easily separate the adsorbents from water after phosphate removal. PSf is widely used as an ultrafiltration membrane and a supporting layer for pervaporation membranes due to its good thermal and chemical stabilities (Kim *et al.* 2002). However, the hydrophobicity of PSf limits its application in water treatment, and thus, a hydrophilic modification must be conducted via blending with other polymeric materials or oxidation (Mok *et al.* 1994). Polyethyleneglycol (PEG) is well known for its hydrophilicity and as a pore-forming agent (Shieh *et al.* 2001, Ma *et al.* 2011).

The objective of this study is to synthesize PSf beads by impregnating different sepiolite ratios with a PSf dope solution and to investigate the characteristics of phosphate adsorption on sepiolite-impregnated PSf beads. The physical and chemical properties of sepiolite-impregnated PSf beads were elucidated. Phosphate adsorption onto the sepiolite-impregnated beads was characterized through batch and fixed-bed column experiments. The batch experiments were performed at different reaction times, initial concentrations, reaction temperatures, pH, and competing anions. The column experiments were performed to assess the applicability of sepiolite-impregnated beads as filter media for 8000 min.

2. Materials and methods

2.1 Preparation and characterization of sepiolite-impregnated PSf beads

In this study, the polymeric materials used in the bead manufacturing process, PSf (P-3500 LCD MB7, Belgium), PEG (Mw = 600 g/mol, Japan), and N-methyl-2-pyrrolidone (NMP, anhydrous, 99.5%, Korea), were purchased from Solvay (Belgium), Tokyo Chemical Industry (Japan), and Daejung Industry Company (Korea), respectively. The natural mineral sepiolite ($\text{Mg}_4(\text{Si}_2\text{O}_5)_3(\text{OH})_2 \cdot 6\text{H}_2\text{O}$) used in this study was purchased from Daeun Chemicals (Incheon, Korea). The size of the sepiolite informed by the manufacturer was 75 μm . Heat treatment was conducted using a tube furnace (5.5 cm in diameter and 55 cm in length) at 900°C, which exhibited the highest phosphate removal efficiency based on the heat treatment of sepiolite for 4 h. The temperature was set according to the literature (Yin *et al.* 2013). The polymer solution was prepared by dissolving PSf in NMP at a ratio of 10:80 (w/w), and thereafter, 10 wt% of PEG was added

to the PSf dissolved in NMP (10:80 w/w) to achieve 100 wt%. To prepare the polymer beads according to the sepiolite impregnation ratios, 10%, 20%, 30%, and 40% of sepiolite were each added to the PSf dope solution. The mixture of sepiolite and the PSf dope solution was intensively stirred at 50°C for 24 h to obtain a homogenous suspension. The beads were prepared by dropping the sepiolite-inclusive dope solution using a syringe equipped with a silicone tube (internal diameter of 4 mm) and a syringe pump (KDS-100, KD Scientific, Korea). The synthesized beads were air-dried for 2 h prior to their use.

For the analysis of the particle surface characteristics of the polymer beads, a field emission scanning electron microscope (FESEM, S4700, Hitachi, Japan) was used. The Fourier transform infrared (FT-IR) spectra of the unmodified PSf bead and 30SPL-PSf bead were analyzed using a Thermo Scientific Instrument (Nicolet 8700) in the wave-number range of 400–4000 cm^{-1} .

2.2 Adsorption experiments

The phosphate adsorption amount of the sepiolite-impregnated PSf beads with different percentages (10%, 20%, 30%, and 40%) of impregnated sepiolite were compared under batch conditions. The batch experiments were conducted as follows: 30 mL of a 200 $\text{mg-PO}_4/\text{L}$ phosphate solution was reacted with 0.1 g of sepiolite-impregnated PSf beads under 160 rpm for 24 h at 25°C. Phosphate solutions were prepared by mixing potassium hydrogen phosphate (K_2HPO_4) and potassium dihydrogen phosphate (KH_2PO_4) in a 1:1 molar ratio. After the reaction, the phosphate solution was separated from the polymer beads by filtration using a filter paper (0.45 μm , Whatman, USA). The phosphate concentration of the filtered solution was measured at a wavelength of 880 nm according to the ascorbic acid reduction method using an ultraviolet-visible (UV-Vis) spectrophotometer (UV-1201, Shimadzu, Japan). All the batch experiments were performed in triplicate.

Kinetic, equilibrium, and thermodynamic adsorption experiments were performed using PSf beads impregnated with 30% sepiolite (30SPL-PSf bead), which was found to be most effective for phosphate removal. The kinetic adsorption experiments were carried out by mixing 0.1 g of the 30SPL-PSf bead and 30 mL of the 200 $\text{mg-PO}_4/\text{L}$ phosphate solution at 160 rpm and 25°C. The reaction times were 0.25, 0.5, 1, 2, 3, 6, 12, 24, and 48 h for the kinetic experiment. The equilibrium adsorption experiments were performed under the same conditions as the kinetic adsorption experiments; however, the initial phosphate concentrations were set at 5, 10, 25, 50, 100, 200, and 500 $\text{mg-PO}_4/\text{L}$. The thermodynamic adsorption experiments were carried out at 15°C, 25°C, and 35°C to investigate the temperature-based phosphate removal characteristics of the 30SPL-PSf bead. Further experiments were performed for phosphate adsorption onto the 30SPL-PSf bead at different pH values and in the presence of anions. The pH of the solution was adjusted to pH 3, 5, 7, 9, and 11 with 0.1 M NaOH and 0.1 M HCl, and the pH was measured using a pH meter (9107BN; Thermo Scientific, USA). To investigate the effect of the competitive anion on the

phosphate adsorption by the 30SPL-PSf bead, the experiments were carried out by adding 1 mM and 10 mM NaNO_3 , Na_2SO_4 , and NaHCO_3 to the 200 mg- PO_4/L phosphate solution.

2.3 Column experiment

Column experiments were performed to compare the phosphate removal using the PSf beads without sepiolite impregnation (0% sepiolite) and the 30SPL-PSf beads under dynamic flow conditions. A Plexiglas (polyethylene) column with an internal diameter of 1.5 cm and a length of 10 cm was used in this study. The water sample used in this study was obtained at Mansu Lake in Korea. According to the water quality standards for lakes established by the Korean Ministry of Environment, the water collected from the Mansu Lake had a high concentration of SS, T-N, T-P, and COD, corresponding to Level 6 (worst water quality level). The lake water had high concentrations of nitrogen and phosphorus due to the influx of a pollutant owing to rainfall runoff from pig farms and agricultural upland near the lake (Gu *et al.* 2017). KH_2PO_4 was added to the lake water to adjust the solution to 5 mg- PO_4/L . Prior to the experiments, the packed column was flushed upward with deionized water using a HPLC pump (Series II pump, Scientific Systems Inc., State College, PA, USA) operating at a rate of 0.3 mL/min until a steady-state flow condition was established. Thereafter, the prepared lake water was introduced into the packed column at the same flow rate, and the column experiment was run for 8000 min. The effluent from the column was collected using a fraction collector (Retriever 500, Teledyne, CA, USA) at a regular interval, and phosphate was analyzed by the ascorbic acid method as described above.

2.4 Data analysis

The kinetic adsorption experiments for the 30SPL-PSf bead were analyzed using pseudo-first-order and pseudo-second-order models:

$$q_t = q_e(1 - e^{-k_1 t}) \quad (1)$$

$$q_t = \frac{k_2 q_e^2 t}{1 + k_2 q_e t} \quad (2)$$

where q_t is the amount of phosphate removed at time t (mg- PO_4/g), q_e is the amount of phosphate removed at equilibrium (mg- PO_4/g), k_1 is the pseudo-first-order rate constant (1/h), and k_2 is the pseudo-second-order rate constant (g/mg- PO_4/h).

The equilibrium data can be analyzed using the Langmuir (Eq. 3) and Freundlich (Eq. 4) models:

$$q_e = \frac{Q_m K_L C}{1 + K_L C} \quad (3)$$

$$q_e = K_F C_e^{\frac{1}{n}} \quad (4)$$

where C is the phosphate concentration in the aqueous solution at equilibrium (mg- PO_4/g), K_L is the Langmuir constant related to the binding energy (L/mg- PO_4), Q_m is the maximum mass of phosphate removed per unit mass of

30SPL-PSf bead (removal capacity of the 30SPL-PSf bead) (mg- PO_4/g), K_F is the distribution coefficient (L/g), and n is the Freundlich constant. The values of K_L , Q_m , K_F , and n can be determined by fitting the Langmuir and Freundlich models to the observed data.

The thermodynamic properties of the experimental results were analyzed using the following equations:

$$\Delta G^0 = \Delta H^0 - T\Delta S^0 \quad (5)$$

$$\Delta G^0 = -RT \ln K_e \quad (6)$$

$$\ln K_e = \frac{\Delta S^0}{R} - \frac{\Delta H^0}{RT} \quad (7)$$

$$K_e = \frac{\alpha q_e}{C_e} \quad (8)$$

where ΔG^0 is the change in Gibb's free energy, ΔS^0 is the change in entropy, ΔH^0 is the change in enthalpy, R is the gas constant, T is the absolute temperature, K_e is the equilibrium constant, and α is the amount of adsorbent.

The total amount of phosphate injected into the column was calculated from the following equation:

$$m_{total} = \frac{C_o Q t_{total}}{1000}, \quad (9)$$

where C_o is the flux concentration of the phosphate, Q is the volumetric flow rate, and t_{total} is the total injection time. The total amount of phosphate removed in the column (q_{total}) when the phosphate concentration and flow rate are constant can be expressed as follows:

$$q_{total} = \frac{Q}{1000} \int_{t=0}^{t=t_{total}} (C_o - C_t) dt, \quad (10)$$

where C_t represents the concentration of the phosphate released at time t . The phosphate removal rate (R_e) of the column during the experiment and the phosphate removal amount (q_a) per unit mass of the filter medium were calculated using the following equation:

$$R_e = \left(\frac{q_{total}}{m_{total}} \right) \times 100, \quad (11)$$

$$q_a = \frac{q_{total}}{x}, \quad (12)$$

3. Results and discussion

3.1 Physical-chemical properties and phosphate removal of sepiolite-impregnated PSf beads

FESEM images of the PSf beads without sepiolite and sepiolite-impregnated PSf beads with different ratios of sepiolite are shown in Fig. 1. The PSf beads have porous honeycomb-like structures (Fig. 1(a)) and the cross-sectional image of the PSf beads shows that the beads had vacant cores (Fig. 1(b)). The PSf beads with 10%, 20%, and 30% sepiolite impregnation also had porous structures and vacant cores (Figs. 1(c)–(h)). However, rod-shaped fibers (sepiolite) were observed in the 40% sepiolite-impregnated PSf beads (Fig. 1(i)), and it had a smaller vacant core than those of the other sepiolite-impregnated PSf beads (Fig. 1(j)).

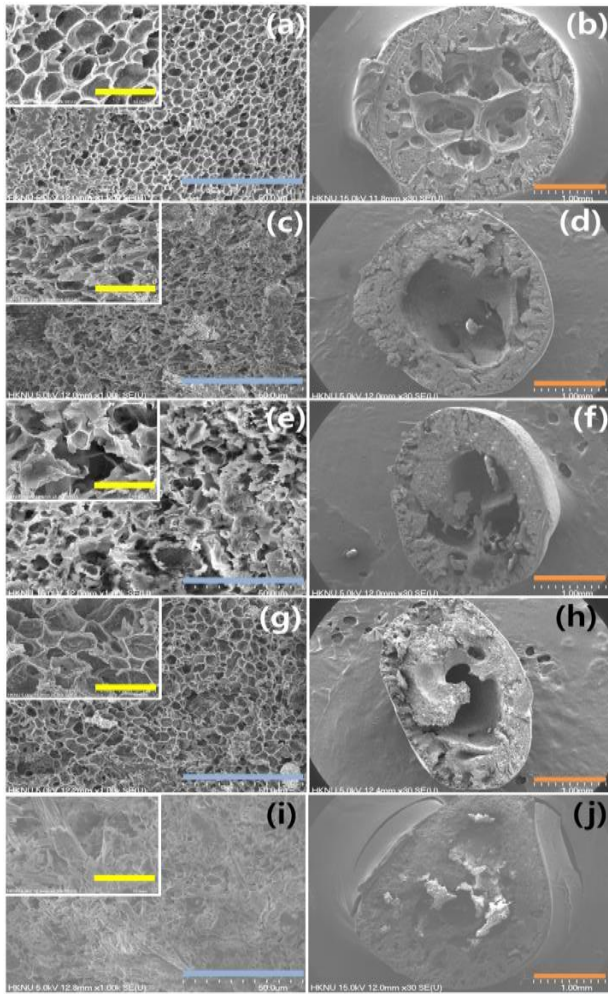


Fig. 1 Cross-sectional images of (a, b) none sepiolite-impregnated PSf bead, (c, d) 10% sepiolite-impregnated PSf bead, (e, f) 20% sepiolite-impregnated PSf bead, (g, h) 30% sepiolite-impregnated PSf bead, and (i, j) 40% sepiolite-impregnated PSf bead by FESEM. Bar scale for the yellow bar: 10 μm , blue bar: 50 μm , and orange bar: 1 mm. Magnification for the left corner: $\times 5000$, left column: $\times 1000$, and right column $\times 30$

The results of the FT-IR analysis of the PSf and 30SPL-PSf beads are shown in Fig. 2. The broad bands at 3469 cm^{-1} and 3415 cm^{-1} of these beads were assigned to OH stretching. The bands visualized in the spectrum at 2924, 1368, and 1160 cm^{-1} correspond to the saturated and unsaturated -CH, aromatic benzene rings, and stretching vibrations of S=O functional groups and ether-O-groups available in the PSf bead (Yurekli 2016). The bands at 1629 cm^{-1} of the 30SPL-PSf bead are characteristic of OH stretching vibrations of hydrated aluminum-magnesium silicate mineral structural OH groups (Yin *et al.* 2013, Navarro *et al.* 2010, Dikmen *et al.* 2011, Liang *et al.* 2013). The characteristic bands of silicate minerals are observed at 1400 cm^{-1} , 1070 cm^{-1} , 974 cm^{-1} (Dikmen *et al.* 2011, Liang *et al.* 2013).

The phosphate removal with PSf beads impregnated with different amounts of sepiolite is shown in Fig. 3. As the impregnated sepiolite amount increased from 10% to

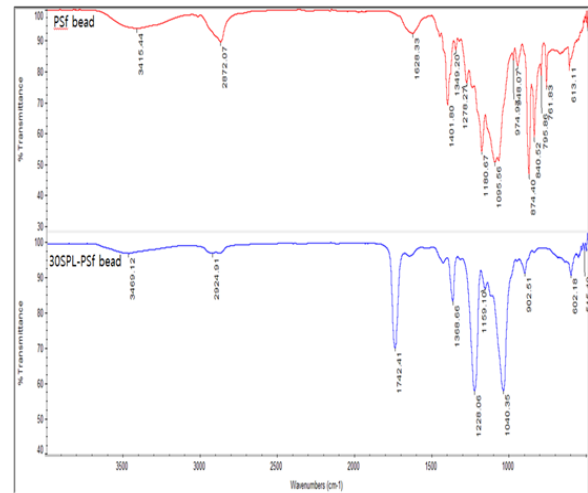


Fig. 2 FTIR-attenuated total reflection spectra of the PSf bead and 30SPL-PSf bead

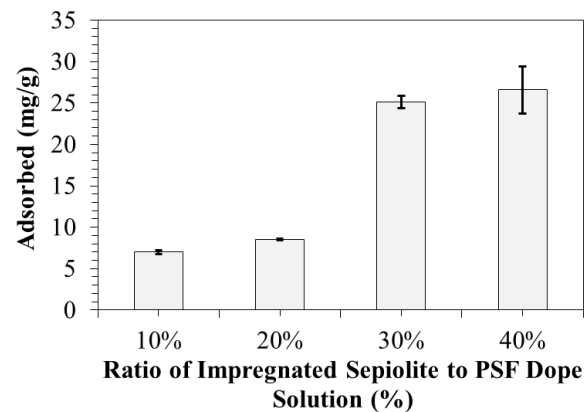


Fig. 3 Effect of the ratio of impregnated sepiolite amount to PSf dope on the phosphate removal by the sepiolite-impregnated PSf beads (initial phosphate concentration: 200 mg/L, pH: 7.0, 30SPL-PSf dosage: 0.1 g, reaction time: 24 h, agitation speed: 160 rpm, and temperature: 25°C)

30%, the amounts of phosphate adsorbed on the PSf beads increased from 6.99 to 25.08 $\text{mg-PO}_4/\text{g}$. The increase in the impregnated sepiolite amount resulted in an increase in the phosphate removal amount. The calcium ions eluted from sepiolite can contribute to the formation of insoluble precipitates, such as $\text{Ca}_5(\text{PO}_4)_3\text{OH}$, $\text{Ca}_2\text{HPO}_4(\text{OH})_2$, $\text{CaHPO}_4 \cdot 2\text{H}_2\text{O}$, and $\text{Ca}_3(\text{HCO}_3)_3\text{PO}_4$, with phosphorus (Cassagne *et al.* 2000, Berg *et al.* 2004, Peng *et al.* 2007). However, the difference between the adsorbed phosphate amount of the 30% and 40% sepiolite-impregnated PSf beads was not significant. It can be explained by the fact that the 40% sepiolite-impregnated PSf beads had relatively small vacant cores and the sepiolite present in the beads was not available for phosphate adsorption.

3.2 Kinetic, isotherm, and thermodynamic studies for phosphate adsorption onto the 30SPL-PSf bead

The results of the 30SPL-PSf bead for phosphate adsorption as a function of reaction time are shown in Fig.

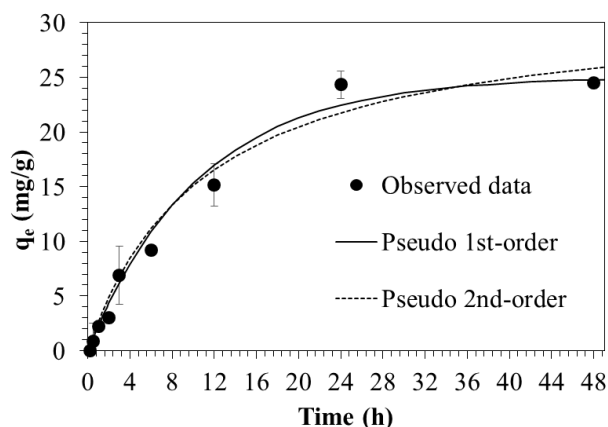


Fig. 4 Kinetic adsorption experiment data with model fittings of the pseudo first-order and pseudo second-order kinetic models for the adsorption of phosphate onto the 30SPL-PSf bead (initial phosphate concentration: 200 mg/L; pH: 7.0; 30SPL-PSf bead dosage: 0.1 g; reaction times: 0.25, 0.5, 1, 2, 3, 6, 12, 24, and 48 h; agitation speed: 160 rpm; temperature: 25°C)

Table 1 Kinetic model parameters obtained from the model fitting of the experimental data

Observed data q_e (mg-PO ₄ /g)	Pseudo-first-order kinetic model parameters			Pseudo-second-order kinetic model parameters		
	q_e (mg-PO ₄ /g)	k_1 (1/h)	R^2	q_e (mg-PO ₄ /g)	k_2 (g/mg/h)	R^2
24.77	25.03	0.09	0.981	31.74	0.01	0.978

4. Table 1 shows the parameters obtained from the pseudo-first-order and pseudo-second-order models. The adsorbed amount of phosphate increased linearly as the reaction time increased until 24 h. The adsorbed phosphate as a function of the reaction time did not show a change in the phosphate adsorption after 24 h, indicating that equilibrium was reached after 24 h. Although the two kinetic models overlapped at a low phosphate concentration, the adsorbed phosphate predicted by the two models displayed a discrepancy at a high phosphate concentration. The determination coefficients (R^2) of the pseudo-first-order and pseudo-second-order models were 0.981 and 0.978, respectively, which are close to unity. The adsorbed phosphate at equilibrium (q_e) of the pseudo-first-order model was 25.03 mg-PO₄/g, which is less than that of the pseudo-second-order model (31.74 mg-PO₄/g) and closer to the experimental data (24.77 mg-PO₄/g). The first-order model described the observed data obtained at different reaction times better than the pseudo-second-order model, indicating that the adsorption rate of phosphate onto the 30SPL-PSf bead is mainly limited by physical diffusion within the particles (Bulut *et al.* 2008, Simonin 2016).

Fig. 5 shows the results of the equilibrium adsorption experiment according to the phosphate concentration in the aqueous solution. The model parameters associated with the adsorption model are shown in Table 2. In the Freundlich

Table 2 Equilibrium model parameters obtained from the model fitting of the experimental data

Model	Parameters		R^2
Langmuir	Q_m (mg-PO ₄ /g) 24.48	K_L (L/mg) 0.42	0.963
Freundlich	K_F (L/g) 10.05	$1/n$ 0.17	0.884

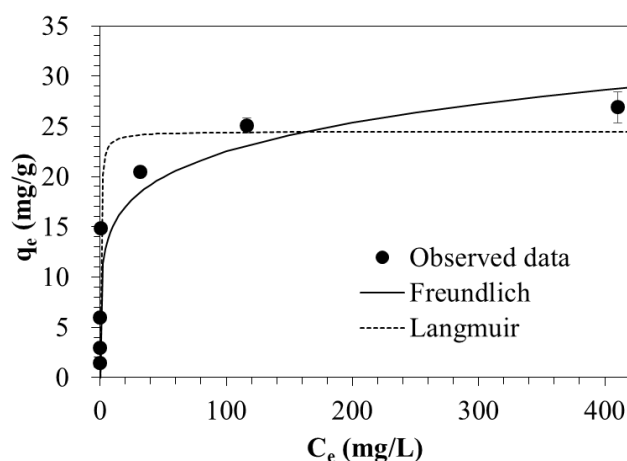


Fig. 5 Equilibrium adsorption experiment data with model fittings of the Freundlich and Langmuir isotherms for the adsorption of phosphate onto the 30SPL-PSf bead (initial phosphate concentrations: 5, 10, 50, 100, 200, and 500 mg/L; pH: 7.0; 30SPL-PSf bead dosage: 0.1 g; reaction time: 24 h; agitation speed: 160 rpm; temperature: 25°C)

model, the partition coefficient (K_F) was 10.05 L/g-PO₄ and the Freundlich constant ($1/n$) was 0.175, which is less than 0.5, indicating that the binding between phosphate and the 30SPL-PSf bead was strong (Summers *et al.* 2011). The Langmuir constant (K_L) in the Langmuir model was 0.421 L/mg-PO₄ and the maximum adsorption capacity (Q_m) was 24.48 mg-PO₄/g. The correlation coefficient, R^2 (0.963), of the Langmuir model is larger than the correlation coefficient, R^2 (0.884), of the Freundlich model, indicating that the Langmuir isotherm is more appropriate for explaining the experimental results. Therefore, it can be concluded that the phosphate adsorption onto the 30SPL-PSf bead is a single-layer adsorption rather than a multi-layer adsorption (Hui *et al.* 2005).

The maximum adsorption capacity of the 30SPL-PSf bead was compared to that of other adsorbents published in the literature. The results show that the 30SPL-PSf beads have a higher adsorption capacity for phosphate than some of the inorganic core material-impregnated polymer beads, such as layered double hydroxide in polyvinyl alcohol/alginate hydrogel beads (1.19 mg-PO₄/g) (Han *et al.* 2012), Mg-Al layered double hydroxide in alginate beads (3.18 mg-PO₄/g) (Han *et al.* 2011), hydrogel chitosan bead (3.34 mg-PO₄/g) (An, 2018), and layered double hydroxide in polyvinylidene fluoride beads (6.28 mg-PO₄/g) (Kim *et al.* 2019).

Table 3 Thermodynamic parameters for phosphate adsorption onto the 30SPL-PSf bead

Temperature (°C)	ΔH° (kJ/mol)	ΔS° (J/K mol)	ΔG° (kJ/mol)
15	65.54	215.99	3.3036
25			1.1437
35			-1.0162

To investigate the effect of the reaction temperature on the phosphate adsorption onto the 30SPL-PSf bead and the thermodynamic characteristics of its adsorption, batch experiments were carried out at different reaction temperatures of 15°C, 25°C, and 35°C with an initial phosphate concentration of 200 mg-PO₄/L. The thermodynamic parameters obtained from the experiment are shown in Table 3. The value of ΔH° was 65.54 kJ/mol, indicating a positive value, showing that the phosphate removal with the 30SPL-PSf bead is an endothermic reaction. The ΔS° value was 215.99 J/K·mol, indicating that the level of the disorder increased at the solid and liquid interfaces. The values of ΔG° decreased as the reaction temperature increased, indicating that the adsorption reaction was enhanced by the temperature increase. The ΔG° turned positive to negative at 30.3°C and became negative at 35°C, indicating that the phosphate adsorption onto the 30SPL-PSf bead was spontaneous at 35°C.

3.3 Effects of the solution pH and the competing anion on the phosphate adsorption onto the 30SPL-PSf bead

The effect of the initial solution pH on the phosphate removal by 30SPL-PSf bead is shown in Fig. 6. As the pH increased, the amount of phosphate adsorption decreased. The highest amount of phosphate adsorption onto the 30SPL-PSf bead appeared to be 27.30 mg/g at pH 3, and the amount of phosphate adsorbed decreased from 27.30 mg/g to 21.54 mg/g as the pH increased from 3.0 to 11.0. These results mirrored those of other studies, in which the pH increase negatively affected the phosphate removal by calcium-rich minerals, such as palygorskite (Gan *et al.* 2009), dolomite (Kim *et al.* 2018), and sepiolite (Yin *et al.* 2013). The phenomenon, that the phosphate adsorption is dependent on the pH, can be explained by the dissolution of cations from the adsorbent, surface charge of the adsorbent, and polyprotic nature of phosphate (Gan *et al.* 2009, Chouyyok *et al.* 2010, Yin *et al.* 2011, Yin *et al.* 2013). Relatively high pH values can decrease the amount of soluble Ca²⁺ leaching from adsorbents (Yin *et al.* 2011), whose metal ions can form insoluble Ca-phosphate precipitates by reacting with soluble phosphate ions in water (Barca *et al.* 2012). In addition, as the pH of the solution increased, the surface of the adsorbents became more negatively charged, thereby increasing the electrostatic repulsion between the phosphate ions and the negatively charged surface of the adsorbents. Considering the dissociation constants of phosphoric acid ($pK_{a,1} = 2.15$, $pK_{a,2} = 7.20$, and $pK_{a,3} = 12.33$) and the final pH (11.38–

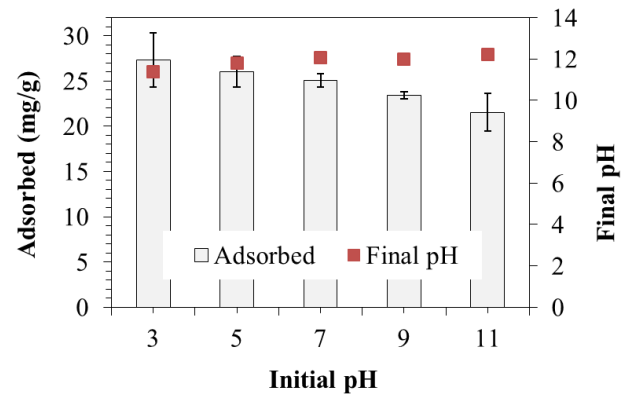


Fig. 6 Effect of the solution pH on phosphate adsorption onto the 30SPL-PSf bead (initial concentration: 200 mg/L, 30SPL-PSf bead dosage: 0.1 g; pH 7; reaction time: 24 h; agitation speed: 160 rpm; temperature: 25°C)

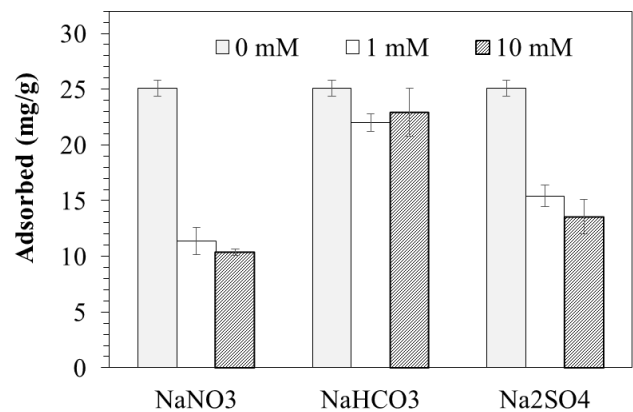


Fig. 7 Effect of the presence of competitive anions (NO₃⁻, HCO₃⁻, SO₄²⁻) on the phosphate adsorption by the 30SPL-PSf bead (initial concentration: 200 mg/L; 30SPL-PSf bead dosage: 0.1 g; pH 7; reaction time: 24 h; agitation speed: 160 rpm; temperature: 25°C)

12.21) of the solution, phosphate ion is mainly present as HPO₄²⁻ with a small amount of PO₄³⁻, leading to it being electrostatically repulsive to negatively charged surfaces (Huang *et al.* 2013).

To investigate the effect of other competitive ions, the results of the 30SPL-PSf bead phosphate adsorption experiment including sulfate ions (SO₄²⁻), bicarbonate ions (HCO₃⁻), and nitrate ions (NO₃⁻) are shown in Fig. 7. In the presence of 1 mM NO₃⁻, HCO₃⁻, and SO₄²⁻, the phosphate unit adsorption amounts were 10.37, 21.98, and 15.43 mg-PO₄/g, respectively. In the presence of 10 mM NO₃⁻, HCO₃⁻, and SO₄²⁻, the amounts of phosphate adsorption greatly decreased to 10.37, 22.94, and 13.56 mg-PO₄/g for NO₃⁻, HCO₃⁻, and SO₄²⁻, respectively. The presence of NO₃⁻ and SO₄²⁻ significantly decreased the amount of phosphate adsorption onto the 30SPL-PSf bead. The impact of HCO₃⁻ on the phosphate adsorption was less than that of NO₃⁻ and SO₄²⁻, because the bicarbonate plays the role of a pH buffer, which inhibits the increase of pH that can make an unfavorable condition for phosphate adsorption.

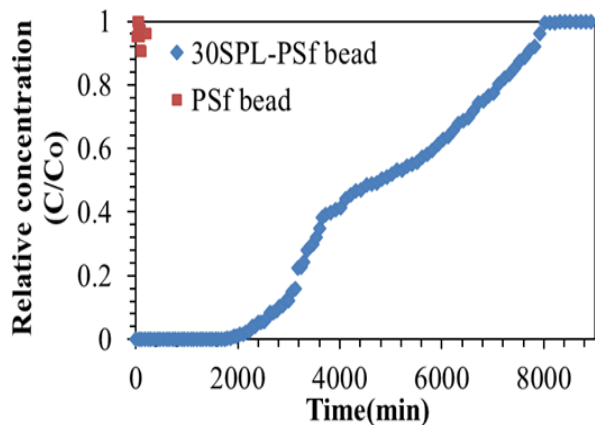


Fig. 8 Breakthrough curves for phosphate removal with the 30SPL-PSf and PSf beads (0% sepiolite)

Table 4 Column experiment results for phosphate removal by the PSf bead (non-impregnated sepiolite) and 30SPL-PSf bead

Filter media	M_{total} (mg-PO ₄)	M_f (g)	q_{total} (mg-PO ₄)	R (%)	q_a (mg-PO ₄ /g)
PSf bead (0% sepiolite)	0.32	3.6	0.025	7.8	0.007
30SPL-PSf bead	12.33	9.8	7.598	61.6	0.775

3.4 Column experiment

For the feasibility test, column experiments were performed using lake water containing the high concentration of SS, T-N, T-P, and COD. The breakthrough curve for phosphate removal in the column packed with PSf beads without sepiolite (PSf beads) and the 30SPL-PSf bead is shown in Fig. 8. The phosphate concentration of the effluent from the column packed with PSf beads reached the initial concentration (5 mg-PO₄/L) in 10 min under the given conditions ($C_0 = 5$ mg-PO₄/L and $Q = 0.3$ mL/min). In the 30SPL-PSf bead, on the other hand, the breakthrough of phosphate began after about 2000 min. After about 8000 min, the phosphate concentration of the effluent reached the influent concentration. Table 4 shows the breakthrough curve analysis parameter according to the column test. The total amount of phosphate removal with the PSf beads (q_{total}) was 0.025 mg-PO₄, and the removal rate (R_e) was 7.8%. The total amount of phosphate removal (q_{total}) was 7.598 mg-PO₄, and the removal rate (R_e) was 61.6% when the 30SPL-PSf beads were used as the filter media. The adsorption amounts per unit mass of adsorbents (q_a) were 0.007 mg-PO₄/g for the PSf beads and 0.775 mg-PO₄/g for the 30SPL-PSf beads. These results indicate that the 30SPL-PSf beads have two orders of magnitude higher efficiency for phosphate removal than that of the PSf beads. The adsorption amount (q_a) (0.775 mg-PO₄/g) of the 30SPL-PSf bead was lower than that of the Langmuir model (Q_m) (24.48 mg-PO₄/g), which is considered to be due to its relatively low initial concentration and short reaction time (32.6 min). The presence of organic matter

and oxyanions in lake water can also contribute lower adsorption of phosphate than synthetic water used in batch equilibrium adsorption experiments (Kim *et al.* 2019).

4. Conclusions

Sepiolite-impregnated PSf beads were synthesized by mixing different ratios (10–40%) of sepiolite in a PSf dope solution. The 30% sepiolite ratio was found to be the most effective for synthesizing the sepiolite-impregnated PSf beads for phosphate removal. The phosphate adsorption onto the 30SPL-PSf beads reached equilibrium in 24 h, and the rate of phosphate adsorption onto the 30SPL-PSf beads was mainly controlled by physical diffusion. The Langmuir model was more suitable for describing the equilibrium adsorption than the Freundlich model, and the phosphate adsorption onto the 30SPL-PSf bead was a single-layer adsorption rather than a multi-layer adsorption. The phosphate adsorption onto the 30SPL-PSf bead was endothermic and spontaneous at 35°C. The increase in the pH of the solution resulted in less phosphate adsorption onto the 30SPL-PSf bead owing to the formation of calcium precipitate with hydroxyl ions and increased the electrostatic repulsion between the phosphate ions and the surface of the 30SPL-PSf bead. Bicarbonate was observed to have less influence on the phosphate removal by the 30SPL-PSf bead than nitrate and sulfate. In the column experiment with the 30SPL-PSf bead, the phosphate in the effluents started to breakthrough after 2000 min of the run, and the phosphate concentration in the effluent reached the influent concentration after about 8000 min of the experimental run. The results of this study show that the impregnation of sepiolite with PSf beads is an easy and effective technique for using sepiolite to separate sepiolite fines after water treatment.

Acknowledgment

This research was supported by Basic Science Research Program through the National Research Foundation of Korea (NRF) funded by the Ministry of Education (No. 2017R1D1A1B03030649).

References

- An, B. (2018), "Removal of both cation and anion pollutant from solution using hydrogel chitosan bead", *J. Korean Soc. Water Wastewater*, **32**(3), 253-259. <https://doi.org/10.11001/jksww.2018.32.3.253>.
- Barca, C., Gérente, C., Meyer, D., Chazarenc, F. and Andrés, Y. (2012), "Phosphate removal from synthetic and real wastewater using steel slags produced in Europe", *Water Res.*, **46**(7), 2376-2384. <https://doi.org/10.1016/j.watres.2012.02.012>.
- Berg, U., Neumann, T., Donnert, D., Nüesch, R. and Stüben, D. (2004), "Sediment capping in eutrophic lakes—efficiency of undisturbed calcite barriers to immobilize phosphorus", *Appl. Geochem.*, **19**(11), 1759-1771. <https://doi.org/10.1016/j.apgeochem.2004.05.004>.
- Bulut, E., Özacar, M. and Şengil, İA (2008), "Equilibrium and kinetic data and process design for adsorption of Congo Red

- onto bentonite”, *J. Hazard. Mater.*, **154**(1-3), 613-622. <https://doi.org/10.1016/j.jhazmat.2007.10.071>.
- Cassagne, N., Remaury, M., Gauquelin, T. and Fabre, A. (2000), “Forms and profile distribution of soil phosphorus in alpine Inceptisols and Spodosols (Pyrenees, France)”, *Geoderma*, **95**(1-2), 161-172. [https://doi.org/10.1016/S0016-7061\(99\)00093-2](https://doi.org/10.1016/S0016-7061(99)00093-2).
- Chouyyok, W., Wiacek, R.J., Pattamakomsan, K., Sangvanich, T., Grudzien, R.M., Fryxell, G.E. and Yantasee, W. (2010), “Phosphate removal by anion binding on functionalized nanoporous sorbents”, *Environ. Sci. Technol.*, **44**(8), 3073-3078. <https://doi.org/10.1021/es100787m>.
- Clark, D., Gu, A.Z. and Neethling, J.B. (2005), “Achieving extremely low effluent phosphorus in wastewater treatment”, *Waterscapes*, **16**(3), 15-17.
- Dikmen, S., Yilmaz, G., Yorukogullari, E. and Korkmaz, E. (2012), “Zeta potential study of natural and acid-activated sepiolites in electrolyte solutions”, *Can. J. Chem. Eng.*, **90**(3), 785-792. <https://doi.org/10.1002/cjce.20573>.
- Gan, F., Zhou, J., Wang, H., Du, C. and Chen, X. (2009), “Removal of phosphate from aqueous solution by thermally treated natural palygorskite”, *Water Res.*, **43**(11), 2907-2915. <https://doi.org/10.1016/j.watres.2009.03.051>.
- Gao, L., Zhang, L., Hou, J., Wei, Q., Fu, F. and Shao, H. (2013), “Decomposition of macroalgal blooms influences phosphorus release from the sediments and implications for coastal restoration in Swan Lake, Shandong, China”, *Ecol. Eng.*, **60**, 19-28. <https://doi.org/10.1016/j.ecoleng.2013.07.055>.
- Gu, B.W., Lee, C.G., Lee, T.G. and Park, S.J. (2017), “Evaluation of sediment capping with activated carbon and nonwoven fabric mat to interrupt nutrient release from lake sediments”, *Sci. Total. Environ.*, **599**, 413-421. <https://doi.org/10.1016/j.scitotenv.2017.04.212>.
- Han, Y.U., Lee, C.G., Park, J.A., Kang, J.K., Lee, I. and Kim, S.B. (2012), “Immobilization of layered double hydroxide into polyvinyl alcohol/alginate hydrogel beads for phosphate removal”, *Environ. Eng. Res.*, **17**(3), 133-138. <https://doi.org/10.4491/eer.2012.17.3.133>.
- Han, Y.U., Lee, W.S., Lee, C.G., Park, S.J., Kim, K.W. and Kim, S.B. (2011), “Entrapment of Mg-Al layered double hydroxide in calcium alginate beads for phosphate removal from aqueous solution”, *Desalin. Water Treat.*, **36**(1-3), 178-186. <https://doi.org/10.5004/dwt.2011.2254>.
- Huang, W.Y., Li, D., Yang, J., Liu, Z.Q., Zhu, Y., Tao, Q., Xu, K., Li, J.Q. and Zhang, Y.M. (2013), “One-pot synthesis of Fe (III)-coordinated diamino-functionalized mesoporous silica: Effect of functionalization degrees on structures and phosphate adsorption”, *Micropor. Mesopor. Mat.*, **170**, 200-210. <https://doi.org/10.1016/j.micromeso.2012.10.027>.
- Hui, K.S., Chao, C.Y.H. and Kot, S.C. (2005), “Removal of mixed heavy metal ions in wastewater by zeolite 4A and residual products from recycled coal fly ash”, *J. Hazard. Mater.*, **127**(1-3), 89-101. <https://doi.org/10.1016/j.jhazmat.2005.06.027>.
- Kang, K., Lee, C.G., Choi, J.W., Hong, S.G. and Park, S.J. (2017), “Application of thermally treated crushed concrete granules for the removal of phosphate: a cheap adsorbent with high adsorption capacity”, *Water Air Soil Poll.*, **228**(1), 8. <https://doi.org/10.1007/s11270-016-3196-1>.
- Kim, J.H., Kang, J.K., Lee, S.C. and Kim, S.B. (2019), “Immobilization of layered double hydroxide in poly (vinylidene fluoride)/poly (vinyl alcohol) polymer matrices to synthesize bead-type adsorbents for phosphate removal from natural water”, *Appl. Clay Sci.*, **170**, 1-12. <https://doi.org/10.1016/j.clay.2019.01.004>.
- Kim, K.S., Lee, K.H., Cho, K. and Park, C.E. (2002), “Surface modification of polysulfone ultrafiltration membrane by oxygen plasma treatment”, *J. Membrane Sci.*, **199**(1-2), 135-145. [https://doi.org/10.1016/S0376-7388\(01\)00686-X](https://doi.org/10.1016/S0376-7388(01)00686-X).
- Kim, M.J., Lee, J.H. and Park, S.J. (2018), “Manufacture of High Efficiency Phosphate Adsorbent by Thermal Treatment of Dolomite”, *KSWST J. Water Treat.*, **26**(1), 69-78.
- Liang, X., Xu, Y., Wang, L., Sun, Y., Lin, D., Sun, Y., Qin, X. and Wan, Q. (2013), “Sorption of Pb²⁺ on mercapto functionalized sepiolite”, *Chemosphere*, **90**(2), 548-555. <https://doi.org/10.1016/j.chemosphere.2012.08.027>.
- Liu, L., Chen, H., Shiko, E., Fan, X., Zhou, Y., Zhang, G., Luo, X. and Hu, X.E. (2018), “Low-cost DETA impregnation of acid-activated sepiolite for CO₂ capture”, *Chem. Eng. J.*, **353**, 940-948. <https://doi.org/10.1016/j.cej.2018.07.086>.
- Loganathan, P., Vigneswaran, S., Kandasamy, J. and Bolan, N.S. (2014), “Removal and recovery of phosphate from water using sorption”, *Crit. Rev. Env. Tec.*, **44**(8), 847-907. <https://doi.org/10.1080/10643389.2012.741311>.
- Ma, Y., Shi, F., Ma, J., Wu, M., Zhang, J. and Gao, C. (2011), “Effect of PEG additive on the morphology and performance of polysulfone ultrafiltration membranes”, *Desalination*, **272**(1-3), 51-58. <https://doi.org/10.1016/j.desal.2010.12.054>.
- Mallin, M.A., Johnson, V.L., Ensign, S.H. and MacPherson, T.A. (2006), “Factors contributing to hypoxia in rivers, lakes, and streams”, *Limnol. Oceanogr.*, **51**(1part2), 690-701. https://doi.org/10.4319/lo.2006.51.1_part_2.0690.
- Mok, S., Worsfold, D.J., Fouda, A. and Matsuura, T. (1994), “Surface modification of polyethersulfone hollow-fiber membranes by γ -ray irradiation”, *J. Appl. Polym.*, **51**(1), 193-199. <https://doi.org/10.1002/app.1994.070510120>.
- Navarro, C., Díaz, M. and Villa-García, M.A. (2010), “Physico-chemical characterization of steel slag. Study of its behavior under simulated environmental conditions”, *Environ. Sci. Technol.*, **44**(14), 5383-5388. <https://doi.org/10.1021/es100690b>.
- Park, S.J., Lee, C.G., Kim, J.H., Kim, S.B., Chang, Y.Y. and Yang, J.K. (2015), “Bimetallic oxide-coated sand filter for simultaneous removal of bacteria, Fe (II), and Mn (II) in small- and pilot-scale column experiments”, *Desalin. Water Treat.*, **54**(12), 3380-3391. <https://doi.org/10.1080/19443994.2014.909333>.
- Peng, J.F., Wang, B.Z., Song, Y.H., Yuan, P. and Liu, Z. (2007), “Adsorption and release of phosphorus in the surface sediment of a wastewater stabilization pond”, *Ecol. Eng.*, **31**(2), 92-97. <https://doi.org/10.1016/j.ecoleng.2007.06.005>.
- Petkuvienė, J., Zilius, M., Lubiene, I., Ruginis, T., Giordani, G., Razinkovas-Baziukas, A. and Bartoli, M. (2016), “Phosphorus cycling in a freshwater estuary impacted by cyanobacterial blooms”, *Estuar. Coasts.*, **39**(5), 1386-1402. <https://doi.org/10.1007/s12237-016-0078-0>.
- Ramasahayam, S.K., Guzman, L., Gunawan, G. and Viswanathan, T. (2014), “A comprehensive review of phosphorus removal technologies and processes”, *J. Macromol. Science, Part A*, **51**(6), 538-545. <https://doi.org/10.1080/10601325.2014.906271>.
- Ruttenberg, K.C. (2003), “The Global Phosphorus Cycle”, *Treatise on Geochemistry*, 585-643. <https://doi.org/10.1016/B0-08-043751-6/08153-6>.
- Shieh, J.J., Chung, T.S., Wang, R., Srinivasan, M.P. and Paul, D.R. (2001), “Gas separation performance of poly (4-vinylpyridine)/polyetherimide composite hollow fibers”, *J. Membrane Sci.*, **182**(1-2), 111-123. [https://doi.org/10.1016/S0376-7388\(00\)00560-3](https://doi.org/10.1016/S0376-7388(00)00560-3).
- Simonin, J.P. (2016), “On the comparison of pseudo-first order and pseudo-second order rate laws in the modeling of adsorption kinetics”, *Chem. Eng. J.*, **300**, 254-263. <https://doi.org/10.1016/j.cej.2016.04.079>.
- Summers, R.S., Knappe, D.R. and Snoeyink, V.L. (2011), “Adsorption of organic compounds by activated carbon”, *Water Quality and Treatment: A Handbook on Drinking Water*, 6th Edition., McGraw-Hill, New York, U.S.A.
- Yin, H., Kong, M. and Fan, C. (2013), “Batch investigations on P

- immobilization from wastewaters and sediment using natural calcium rich sepiolite as a reactive material”, *Water Res.*, **47**(13), 4247-4258. <https://doi.org/10.1016/j.watres.2013.04.044>.
- Yin, H., Yun, Y., Zhang, Y. and Fan, C. (2011), “Phosphate removal from wastewaters by a naturally occurring, calcium-rich sepiolite”, *J. Hazard. Mater.*, **198**, 362-369. <https://doi.org/10.1016/j.jhazmat.2011.10.072>.
- Yurekli, Y. (2016), “Removal of heavy metals in wastewater by using zeolite nano-particles impregnated polysulfone membranes”, *J. Hazard. Mater.*, **309**, 53-64. <https://doi.org/10.1016/j.jhazmat.2016.01.064>.

CC